SHELL EFFECTS IN THE FRAGMENTATION POTENTIAL FOR SUPERHEAVY ELEMENTS

D. ARANGHEL[1,2], A. SANDULESCU[1,3]

[1]"Horia Hulubei" National R&D Institute for Physics and Nuclear Engineering,
Reactorului 30, RO-077125, POB-MG6, Măgurele-Bucharest, Romania
[2]Extreme Light Infrastructure Nuclear Physics (ELI-NP),
Reactorului 30, RO-077125, POB MG-6, Magurele-Bucharest, Romania
[3]Academia Romana, Calea Victoriei 125, Bucharest, Romania

Received July 8, 2014

Investigations of the fragmentation potential energy surface is realized in the frame of the macroscopic-microscopic model in order to emphasize the importance of the shell effects in the synthesis and the stability of superheavy nuclei. The shell effects and the macroscopic potential are reported separately. The origin of several minima that are responsible for metastable states is discussed.

Key words: Macroscopic-microscopic model, shell effects, isomer states, superheavy nuclei.

PACS: 21.60.Cs.

1. INTRODUCTION

The investigations of the fragmentation potential energy surface in the framework of the macroscopic-microscopic model for the formation of the superheavy nucleus ^{296}Lv revealed the formation of several minima [1]. The authors of Ref. [1] considered that these minima are responsible for metastable states that occur during the synthesis of superheavy elements. It is claimed that such states explain the quasi-fission structure distribution obtained during the bombardment of the target with ^{48}Ca projectiles [2]. In order to understand the origin of these isomer minima, the fragmentation potential as function of the mass asymmetry and the elongations is calculated to evidence the importance of the shell effects in the synthesis and the stability of superheavy nuclei. In the following, the macroscopic energy and the microscopic effects are reported separately and their behavior are discussed. In order to compute the total energy of the nuclear system we rely on the macroscopic-microscopic approximation. Within this method, it is assumed that a macroscopic model, as the liquid drop one, describes quantitatively the smooth trends of the potential energy with respect to the particle number and deformation. A microscopic approach is responsible for the local fluctuations. These local fluctuations are calculated with the Strutinsky prescriptions.

It is worth to mention that the stability of the superheavy nuclei was predicted within the macroscopic-microscopic approximation [3]. Later on, the optimum choice of the two partners that collide to form a superheavy nucleus was determined with the fragmentation theory [4] by considering the fusion as a cold rearrangement process. Investigating the total potential energy, it was predicted that the most favorable reactions are connected with the valley of the Pb [5–7]. An analogue most favorable valley was found for cluster decay [8]. In Ref. [6], the ^{48}Ca was proposed as a projectile on various transuranium targets.

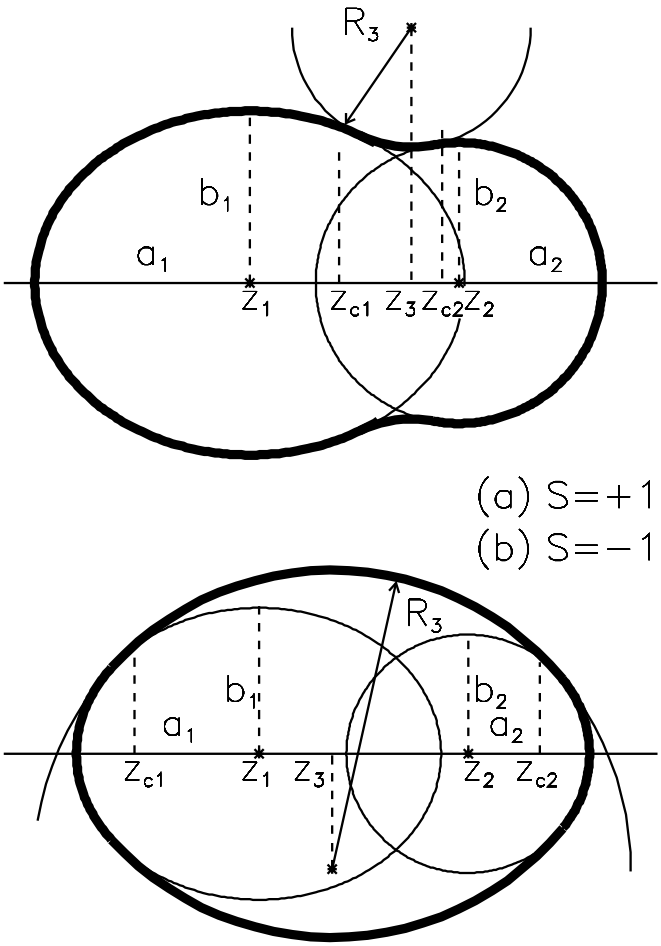

Fig. 1 – Nuclear shape parametrization.

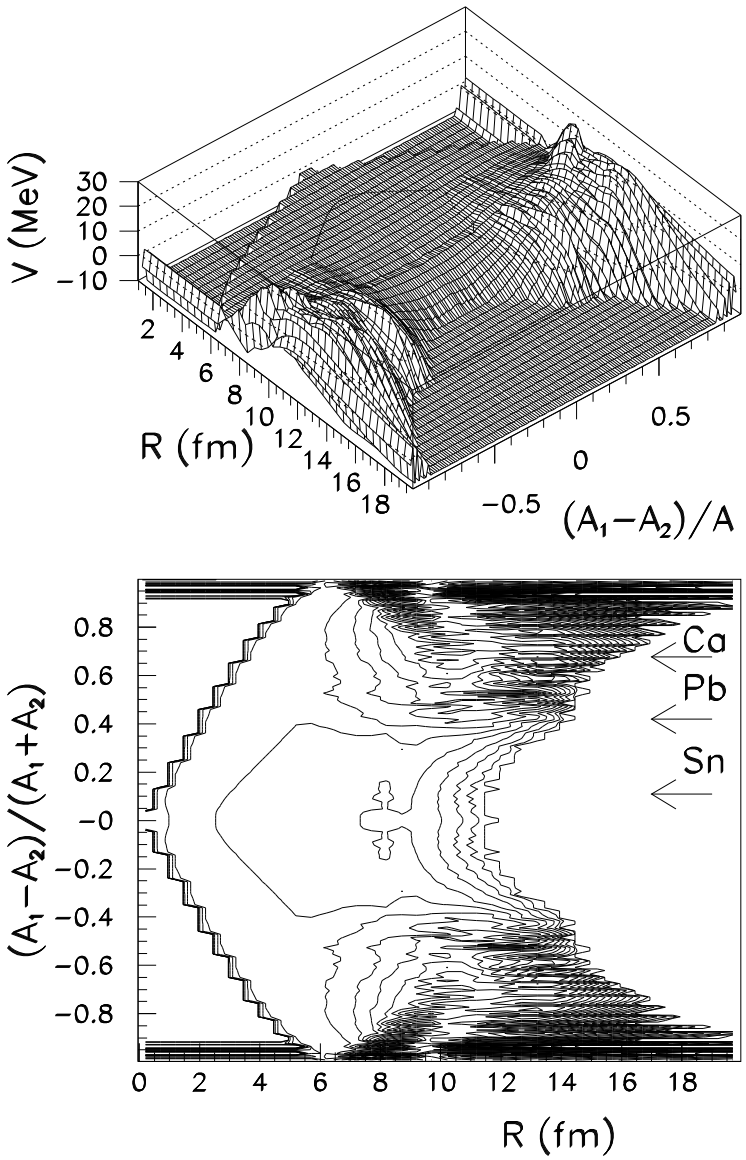

Fig. 2 – The liquid drop potential surface in the mass asymmetry and elongation coordinates. The step between two equipotential lines in the lower panel is 2 MeV. The mass asymmetries corresponding to the Ca, Pb and Sn channels are marked with arrows.

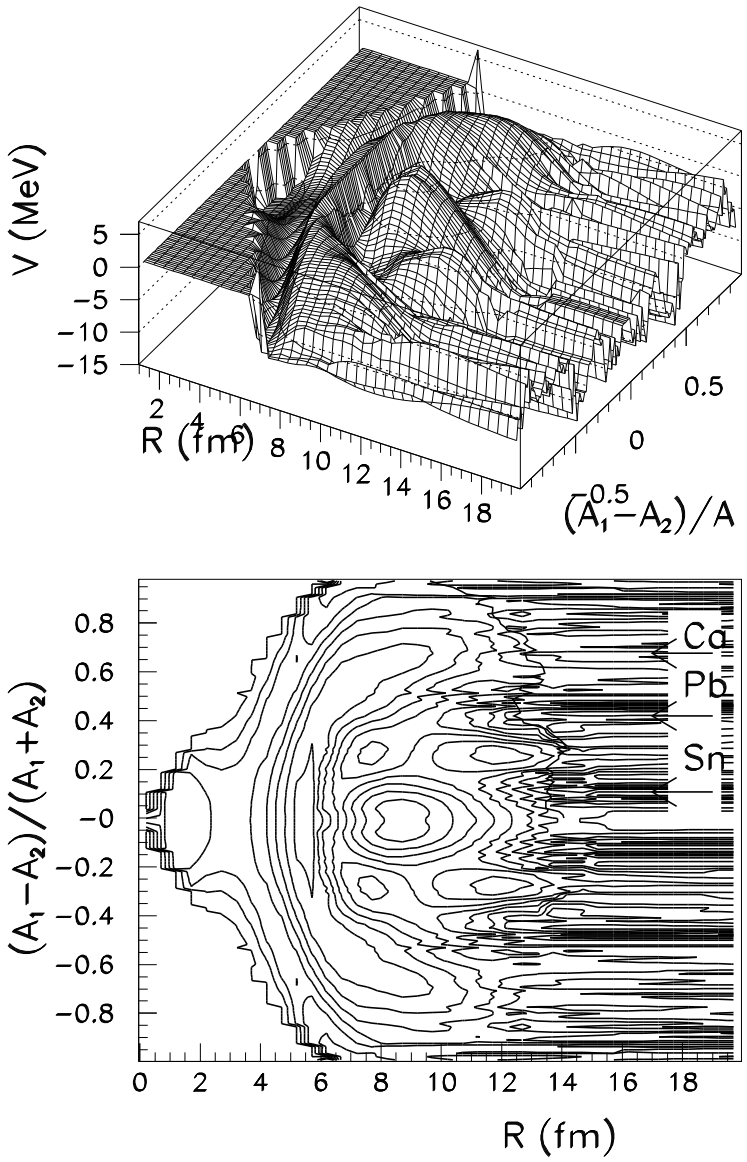

Fig. 3 – The shell and pairing corrections in the mass asymmetry and elongation coordinates. The step between two equipotential lines in the lower panel is 2 MeV.

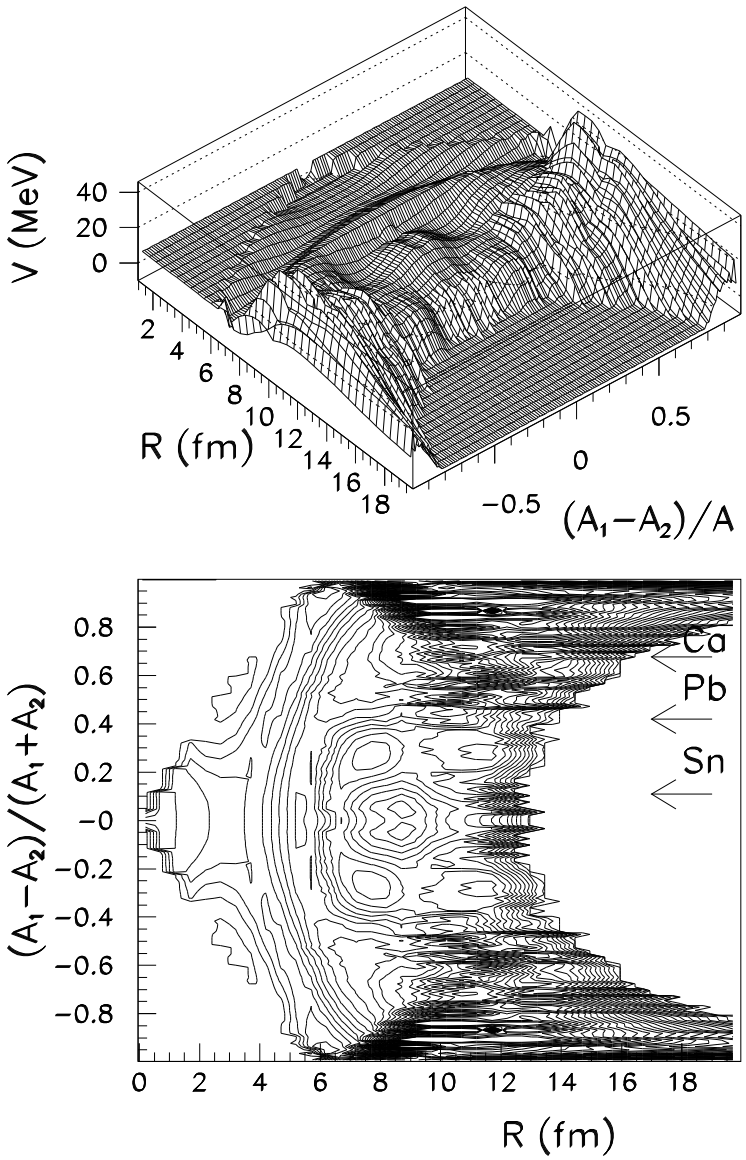

Fig. 4 – Fragmentation potential in the framework of the macroscopic-microscopic model. The step between two equipotential lines in the lower panel is 2 MeV.

2. FORMALISM

In the macroscopic microscopic model [9–11] we must start with the parametrization of the nuclear shape. In the following, a nuclear shape parametrization obtained

by smoothly joining two spheroids of semi-axis a_i and b_i (i=1,2) with a neck surface generated by the rotation of a circle of radius R_3 around the axis of symmetry is used. This parametrization is characterized by five independent generalized coordinates $\{q_i\}$ (i=1,5). The degrees of freedom are the elongation R given by the distance between the centers of the spheroids; the necking parameter $C_3 = S/R_3$ related to the curvature of the neck, the eccentricities $\epsilon_i = \sqrt{1-(b_i/a_i)^2}$ (i=1,2) associated with the deformations of the nascent fragments and the mass asymmetry parameter $\eta = (A_1 - A_2)/(A_1 + A_2)$, where A_1 and A_2 are the mass numbers of the nascent fragments. These numbers are obtained by calculating the virtual volumes of the two ellipsoids with semi-axis a_i and b_i. The nuclear shape is displayed in Fig. 1 where the geometrical parameters could be recognized.

The macroscopic energy (liquid drop one) is obtained in the framework of the Yukawa-plus-exponential model [12] extended for binary systems with different charge densities as detailed in Ref. [13, 14]. The parameters of the model are taken from Ref. [15]. The macroscopic energy contains several terms: the surface energy, the Coulomb energy and its diffusivity, the volume energy, the Wigner term and the A_0-one. When the the nucleus changes the deformation, the single particle levels are rearranged. As mentioned, the internal structure of the nucleus is translated in shell and pairing corrections within the Strutinsky prescriptions. These corrections are added to the to the liquid drop energy. Therefore, the total potential is modulated by these corrections. The Strutinsky procedure as described in Ref. [11] was used. These corrections represent the varying parts of the total binding energy caused by the shell structure. The single-particle-level diagrams are computed within the Woods-Saxon superasymmetric two- center shell model [22]. The Woods-Saxon potential, the spin-orbit term and the electrostatic potential are diagonalized within the two-center semi-symmetric oscillator wave functions [16–19]. This parametrization was widely used by the Bucharest group in the calculations addressing the cluster and alpha decay [20–26], the fission [27–32] and its dissipation, the pair breaking [33, 34], the generalization of time dependent pairing equations [22], the heavy element synthesis [35, 36], and the double beta decay [37]. Being able to treat extreme asymmetries of the fission process, the two center approach emerges as a competitive model for the alpha decay which is usually treated with preformation models [38, 39].

3. RESULTS

The best target/projectile combinations for the formation of the $^{296}116$ superheavy element are tested. For this purpose, the ground state eccentricities ϵ_i (i=1,2) are calculated for the nuclei A_1 and A_2 that can be used as partners in the reaction $^{A_1}Z_1 + ^{A_2}Z_2 = ^{296}116$. All this combinations were tested in the touching configura-

tion. The combination that gives the lowest total energy was retained for each mass asymmetry. The path in the multidimensional configuration was used for the family of nuclear shapes that begins from the ground state and reach the scission point, as described in Ref. [1].

In the Fig. 2, the energy surface for the liquid drop potential is displayed as function of the mass asymmetry $\eta = (A_1 - A_2)/(A_1 + A_2)$ and the elongation R coordinates. The spherical shape corresponds to the asymmetry $\eta = 0$ and the elongation R=0 fm. When the distance between the nascent fragments increases, the two nuclei reach their individualities. For mass asymmetries close to $\eta \approx 0$ (symmetric fission) the macroscopic barrier is practically non existent. In these conditions, the Z=116 compound nucleus cannot survive. The main decay process predicted by the liquid drop model is therefore the fission. The potential energy surface exhibits two maxima for mass asymmetries close to $\eta = \pm 0.9$. As expected, the deep minimum at symmetry is flanked by the Businaro-Gallone mountains, responsible for the macroscopic barriers in the region of the scission configuration. The α-decay proceeds through a path that arrives close to $\eta = \pm 1$, for values of the mass asymmetries larger than the the maximal values of the Businaro-Gallone mountains.

The structure of the compound nucleus plays a major role in its stability. The internal structure is translated in shell and pairing effects that should be added to the liquid drop energy in the framework of the macroscopic-microscopic model. In Fig. 3, the shell and pairing corrections are plotted *versus* the mass asymmetry and the elongation. In general, the minimal values of the microscopic corrections reveal the existence of some gaps in the single particle levels schemes around the Fermi energy. Such minima can be observed in Fig. 3 for the spherical configuration and around the values $\eta = \pm 0.3$ and $R \approx 7.7$ fm. It is interesting to note that some well behaved valleys could be observed in the external region (i.e., large values of the elongation R) for target/projectile combinations in which one of the nuclei is Ca, Pb or Sn. These nuclei are characterized by magic numbers of nucleons and their binding energy is larger. One of these valleys is continued deeply in the overlapping region of the fragments up to $R \approx 8$ fm, close to the mass asymmetry $\eta = 0.5$. Another minimum is also visible for the formation of the alpha decay on the surface ($\eta \approx \pm\ 1$ and $R \approx 6$ fm). The importance of this minimum was investigated in Ref. [20]. It is worth to mention that the preformation model of alpha decay also predicts the existence of isomeric excited states for superheavy nuclei [40].

In Fig. 4, the macroscopic-microscopic energy is displayed. The two Businaro-Gallone are still existent for large values of the mass asymmetries. However, a barrier is now present between the spherical ground state of the parent (R=0 fm) and the external region. This barrier is given by shell effects and it is responsible for the stability of the superheavy nucleus. Due to this barrier, the probability that the compound superheavy nucleus decay through fission is very small. The minimum

for $\eta = \pm 0.3$ and $R \approx 7$ fm is due to the pronounced shell effects revealed in Fig. 3. Another minimum for $\eta = \pm 0.48$ and R=8.6 fm is due to the valley that belongs to the Pb partner as discussed above. This valley is continued in the external region of the two fragments. However, this valley is crossed by the macroscopic barrier in the vicinity of the scission, creating a metastable minimum in the potential energy surface. In this way several minima in the potential energy landscape are created at different values of the mass asymmetry. These minima can be responsible for the structure observed for the quasifission cross section process as mentioned in Ref. [1].

In conclusion, the metastable states of the superheavy elements are mainly due to the interplay between the macroscopic energy and the shell effects. In the case of the metastable state located at a large mass asymmetry $\eta = \pm$ 0.48, an influence of the double magic Pb partner can be envisaged. The calculations were made by inferring the ground state configurations of the partners. Therefore, the fission from spherical ground state can be considered as a cold process. In this context, the fission must surpass a very high barrier due to the shell effects and the cold fission process is not too probable.

Acknowledgements. We thank to M. Mirea for providing us the two center Woods-Saxon codes. Work supported by CNCS - UEFISCDI, project number PN - II - ID - PCE - 2011 -3 - 0068.

REFERENCES

1. A. Sandulescu and M. Mirea, Eur. Phys. J. A **50**, 110 (2014).
2. M.G. Itkis, A.A. Bogachev, I.M. Itkis, G.N. Knyazheva, N.A. Kondratiev, E.M. Kozulin, L. Krupa, Yu.Ts. Oganessian, I.V. Pokrovsky, E.V. Prokhorova, A.Ya. Rusanov, V.M. Voskresenski, V.A. Rubchenya and W.H. Trzaska, Int. J. Mod. Phys. E **16**, 957 (2007).
3. A. Sobiczewski and K. Pomorski, Prog. Part. Nucl. Phys. **58**, 292 (2007).
4. A. Sandulescu, R.K. Gupta, W. Scheid and W. Greiner, Phys. Lett. B **60**, 225 (1976).
5. R.K. Gupta, C. Parvulescu, A. Sandulescu and W. Greiner, Z. Phys. A **283**, 217 (1977).
6. R.K. Gupta, A. Sandulescu and W. Greiner, Phys. Lett. B **67**, 257 (1977).
7. R.K. Gupta, A. Sandulescu and W. Greiner, Z. Naturforsch **32a**, 704 (1977).
8. A. Sandulescu, D.N. Poenaru and W. Greiner, Sov. J. Part. Nucl. **11**, 528 (1980).
9. J.R. Nix, Ann. Rev. Nucl. Sci. **22**, 65 (1972).
10. W.J. Swiatecki and S. Bjornholm, Phys. Rep. **4**, 325 (1972).
11. M. Brack, J. Damgaard, A.S. Jensen, H.C. Pauli, V.M. Strutinsky and C.Y. Wong, Rev. Mod. Phys. **44**, 320 (1972).
12. K.T.R. Davies and J.R. Nix, Phys. Rev. C **14**, 1977 (1976).
13. M. Mirea, O. Bajeat, F. Clapier, F. Ibrahim, A.C. Mueller, N. Pauwels and J. Proust, Eur. Phys. J. A **11**, 59 (2001).
14. D.N. Poenaru, M. Ivascu and D. Mazilu, Comput. Phys. Commun. **19**, 205 (1980).
15. P. Moller, J.R. Nix, W.D. Myers and W.J. Swiatecki, Atom. Data Nucl. Data Tabl. **59**, 185 (1995).
16. E. Badralexe, M. Rizea and A. Sandulescu, Rev. Roum. Phys. **19**, 63 (1974).
17. M. Mirea, Phys. Rev. C **54**, 302 (1996).

18. M. Mirea, Nucl. Phys. A **780**, 13 (2006).
19. J. Maruhn and W. Greiner, Z. Phys. **251**, 431 (1972).
20. A. Sandulescu, M. Mirea and D.S. Delion, EPL **101**, 62001 (2013).
21. M. Mirea, Phys. Rev. C **63**, 034603 (2001).
22. M. Mirea, Phys. Rev. C **78**, 044618 (2008).
23. M. Mirea, A. Sandulescu and D.S. Delion, Nucl. Phys. A **870-871**, 23 (2011).
24. M. Mirea, A. Sandulescu and D.S. Delion, Eur. Phys. J. A **48**, 86 (2012).
25. A. Sandulescu and M. Mirea, Rom. Rep. Phys. **65**, 688 (2013).
26. M. Mirea, Eur. Phys. J. A **4**, 335 (1999).
27. M. Mirea Phys. Rev. C **83**, 054608 (2011).
28. M. Mirea, Phys. Lett. B **717**, 252 (2012).
29. M. Mirea, D.S. Delion and A. Sandulescu, Phys. Rev. C **81**, 044317 (2010).
30. A.-M. Micu and M. Mirea, Rom. J. Phys. **58**, 939 (2013).
31. N.S. Shakib, M.F. Rahimi and M.M. Firoozabadi, Rom. Rep. Phys. **65**, 401 (2013).
32. M. Mirea and R.C. Bobulescu, J. Phys. G. **37**, 055106 (2010).
33. M. Mirea, Phys. Lett. B **680**, 316 (2009).
34. M. Mirea, Phys. Rev. C **89**, 034623 (2014).
35. M. Mirea, D. S. Delion and A. Sandulescu, EPL **85**, 12001 (2009).
36. A. Sandulescu and M. Mirea, Rom. J. Phys. **58**, 1148 (2013).
37. T.E. Pahomi, A. Neacsu, M. Mirea and S. Stoica, Rom. Rep. Phys. **66**, 370 (2014).
38. I. Silisteanu and A.I. Budaca, Rom. J. Phys. **58**, 1198 (2013).
39. I. Silisteanu and A.I. Budaca, Rom. Rep. Phys. **65**, 757 (2013)
40. D.S. Delion, R.J. Liotta and R. Wyss, Phys. Rev. C **76**, 044301 (2007).